GRP1 Pleckstrin Homology Domain: Activation Parameters and Novel Search Mechanism for Rare Target Lipid[†]

John A. Corbin, Ronald A. Dirkx, and Joseph J. Falke*

Molecular Biophysics Program and The Department of Chemistry and Biochemistry, University of Colorado, Boulder, Colorado 80309-0215

Received May 14, 2004; Revised Manuscript Received September 12, 2004

ABSTRACT: Pleckstrin homology (PH) domains play a central role in a wide array of signaling pathways by binding second messenger lipids of the phosphatidylinositol phosphate (PIP) lipid family. A given type of PIP lipid is formed in a specific cellular membrane where it is generally a minor component of the bulk lipid mixture. For example, the signaling lipid PI(3,4,5)P_3 (or PIP_3) is generated primarily in the inner leaflet of the plasma membrane where it is believed to never exceed 0.02% of the bulk lipid. The present study focuses on the PH domain of the general receptor for phosphoinositides, isoform 1 (GRP1), which regulates the actin cytoskeleton in response to PIP_3 signals at the plasma membrane surface. The study systematically analyzes both the equilibrium and kinetic features of GRP1-PH domain binding to its PIP lipid target on a bilayer surface. Equilibrium binding measurements utilizing protein-to-membrane fluorescence resonance energy transfer (FRET) to detect GRP1-PH domain docking to membrane-bound PIP lipids confirm specific binding to PIP_3. A novel FRET competitive binding measurement developed to quantitate docking affinity yields a K_D of 50 ± 10 nM for GRP1-PH domain binding to membrane-bound PIP_3 in a physiological lipid mixture approximating the composition of the plasma membrane inner leaflet. This observed K_D lies in a suitable range for regulation by physiological PIP_3 signals. Interestingly, the affinity of the interaction decreases at least 12-fold when the background anionic lipids phosphatidylserine (PS) and phosphatidylinositol (PI) are removed from the lipid mixture. Stopped-flow kinetic studies using protein-to-membrane FRET to monitor association and dissociation time courses reveal that this affinity decrease arises from a corresponding decrease in the on-rate for GRP1-PH domain docking with little or no change in the off-rate for domain dissociation from membrane-bound PIP_3. Overall, these findings indicate that the PH domain interacts not only with its target lipid, but also with other features of the membrane surface. The results are consistent with a previously undescribed type of two-step search mechanism for lipid binding domains in which weak, nonspecific electrostatic interactions between the PH domain and background anionic lipids facilitate searching of the membrane surface for PIP_3 headgroups, thereby speeding the high-affinity, specific docking of the domain to its rare target lipid.

Many significant events in cell signaling take place at membrane surfaces, particularly at the surface of the plasma membrane where receptors, channels, and signaling complexes make critical decisions to turn specific pathways on or off. An important class of membrane-bound second messengers that often play key roles in such decisions are the phosphatidylinositol phosphate lipids (PIP[1] lipids). Three of the most well characterized PIP signaling lipids in the plasma membrane are PI(3,4,5)P_3, PI(3,4)P_2, and PI(4,5)P_2. These PIP lipids regulate a wide array of cellular pathways and processes including cell growth and chemotaxis, DNA synthesis, vesicle trafficking, cytoskeletal rearrangements, apoptosis, and transformation (for reviews see refs *1*−*6*).

PIP lipid signals are transduced by a ubiquitous class of conserved signaling modules, known as pleckstrin homology or PH domains, that have been identified in over 320 different proteins of the human genome (PFAM database, *7*). An important subset of the PH domains examined to date have been found to exhibit both high affinity and strong selectivity for specific PIP lipids (for reviews see refs *4* and *8*−*12*). PH domains that belong to this high-affinity class of PIP lipid binders play a crucial role in regulating cellular responses to PIP lipid signals with temporal and spatial precision, serving to drive the docking of their parent protein to the appropriate intracellular membrane in response to the

[†] Support provided by NIH Grant GM R01-63235 (to J.J.F.).

* To whom correspondence should be addressed. E-mail falke@colorado.edu; tel 303-492-3597; fax 303-492-5894.

[1] Abbrevations: GRP1, general receptor for phosphoinositides, isoform 1; PLCδ1, phospholipase C δ1; Arf, ADP-ribosylation factor; ARNO, Arf nucleotide-binding site opener; PH domain, pleckstrin homology domain; PI3K, phosphoinositide 3-kinase; PIP, phosphatidylinositol phosphate; PI(3,4,5)P_3 (or PIP_3), phosphatidylinositol 3,4,5-trisphosphate; PI(3,4)P_2, phosphatidylinositol 3,4-bisphosphate; PI(4,5)P_2, phosphatidylinositol 4,5-bisphosphate; I(1,3,4,5)P_4 (or IP_4), D-*myo*-inositol 1,3,4,5-tetrakisphosphate; I(1,2,3,4,5,6)P_6 (or IP_6), D-*myo*-inositol 1,2,3,4,5,6-hexakisphosphate; PC, phosphatidylcholine; PE, phosphatidylethanolamine; dPE (or dansyl-PE), dansyl-phosphatidylethanolamine; PS, phosphatidylserine; PI, phosphatidylinositol; SM, sphingomyelin; FRET, fluorescence resonance energy transfer.

10.1021/bi049017a CCC: $27.50
Published on Web 12/03/2004

localized accumulation of a specific target lipid. Although high-resolution structural studies have provided significant insights into the molecular basis of PIP headgroup recognition by PH domains (*13*−*18*), much remains to be learned about the association of PH domains with PIP lipids on real membrane surfaces. Since target PIP lipids are typically rare molecules comprising a small fraction of the lipids present on membrane surfaces even during a signaling event, a molecular understanding of PH domain function would include a description of search mechanisms used by PH domains to find their rare target lipids in a sea of nontarget lipids.

PH domains share a common structural topology (*4*, *10*). The PH fold, typically 100−120 residues in length, is a sandwich of two β-sheets, one containing four antiparallel β-strands ($\beta1-\beta4$) and the other containing three antiparallel β-strands ($\beta5-\beta7$). A C-terminal amphipathic α-helix lies at one edge of the β-sandwich, while the opposite edge displays three interstrand loops that vary in length between different PH domains. These three loops, known as $\beta1/\beta2$, $\beta3/\beta4$, and $\beta6/\beta7$, have been shown to form a basic binding pocket for the headgroup of a target PIP lipid (*10*), and both the lengths and primary sequences of these loops are specialized to provide the appropriate PIP lipid specificity.

The differing target lipid specificities of PH domains largely define their biological roles in modulating different signaling pathways. PH domains that specifically interact with the signaling lipid PI(3,4,5)P_3 serve as a direct link between a large class of cell surface receptors that activate class I phosphoinositide 3-kinases (PI3Ks) (*5*, *19*, *20*) and downstream signaling events. PI3K-catalyzed formation of PI(3,4,5)P_3 in the plasma membrane has been implicated as the trigger of many crucial cellular signals that regulate cell growth, cell cycle transitions, cell migration, and vesicle trafficking; moreover, defective PI(3,4,5)P_3 signaling has been implicated in human cancers and diabetes (*19*−*24*). On a molecular level, PH domain binding to PI(3,4,5)P_3 targets many signaling enzymes to the plasma membrane surface including GTP/GDP exchange factors, cytoskeleton regulatory proteins, membrane protein kinases, lipid kinases, and other lipid modification enzymes that generate new lipid-derived second messengers. Other PH domains specifically target different PIP lipids (such as PI(3,4)P_2, PI(4,5)P_2, PI(3)P_1, PI(4)P_1, and PI(5)P_1) in various signaling pathways localized to the plasma or internal membranes.

Previous studies, providing much useful information, have analyzed the binding of isolated PH domains and their fusion constructs to soluble PIP lipid analogues or to membrane-bound PIP lipids in monolayers or bilayers (*25*−*38*). However, the present study represents the first combined equilibrium and kinetic analysis of an isolated PH domain docking to its target lipid on the surface of a membrane bilayer. The study focuses on a representative PI(3,4,5)P_3-specific PH domain, namely, that of the general receptor for phosphoinositides, isoform 1 (GRP1). GRP1 is a member of the cytohesin family of GTP/GDP exchange factors (GEFs) that activate ADP ribosylation factors (Arfs) involved in actin reorganization (*39*) in pathways such as chemotaxis (*23*, *24*, *40*, *41*). Structurally, the PH and GEF domains of GRP1 are independent, and membrane binding affinity resides solely in the PH domain, which exhibits high affinity and selectivity for PI(3,4,5)P_3 (*17*, *27*, *31*). The crystal structure of this PH domain has been solved in both apo form and bound to the headgroup analogue I(1,3,4,5)P_4 (or IP_4) (*15*, *17*).

The present analysis begins by measuring the equilibrium dissociation constant (K_D), as well as the kinetic on- and off-rate constants (k_{on}, k_{off}), for the binding of GRP1-PH domain to membrane bilayers composed of both simple and physiological lipid mixtures. Together these measurements provide a systematic equilibrium and kinetic analysis of GRP1-PH domain docking to membrane-bound target lipids, yielding limits on the PI(3,4,5)P_3 concentrations and time scales needed to generate signaling events. Moreover, the results reveal a novel mechanism used by the GRP1-PH domain to search for its rare target lipid on a membrane surface. Overall, the findings provide new insights into PH domain activation parameters and docking mechanism.

EXPERIMENTAL PROCEDURES

Reagents. All lipids were synthetic unless otherwise indicated. 1-Palmitoyl-2-oleoyl-*sn*-glycero-3-phosphocholine (phosphatidylcholine, PC); 1-palmitoyl-2-oleoyl-*sn*-glycero-3-phosphoethanolamine (phosphatidylethanolamine, PE); phosphatidylinositol (PI) natural, bovine liver; 1-palmitoyl-2-oleoyl-*sn*-glycero-3-phosphoserine (phosphatidylserine, PS); and sphingomyelin (SM) natural, brain, were all from Avanti Polar Lipids. Dipalmitoyl D-*myo*-phosphatidylinositol 4,5-bisphosphate (PI(4,5)P_2), dipalmitoyl D-*myo*-phosphatidylinositol 3,4-bisphosphate (PI(3,4)P_2) and dipalmitoyl D-*myo*-phosphatidylinositol 3,4,5-trisphosphate (PI(3,4,5)P_3) were purchased from Echelon Biosciences. The *N*-[5-(dimethylamino)naphthalene-1-sulfonyl]-1,2-dihexadecanoyl-*sn*-glycero-3-phosphoethanolamine (dansyl-PE, dPE) was from Molecular Probes. D-*myo*-Inositol 1,2,3,4,5,6-hexakisphosphate dodecasodium salt (IP_6) was from Calbiochem.

Cloning, Expression and Purification of GRP1-PH Domain. GRP1-PH domain (residues 255−392 of full-length GRP1) was cloned by PCR amplification from the human expressed sequence tag (EST) clone (accession no. BG620295). The PH domain of GRP1 was expressed as a glutathione S-transferase (GST) fusion protein and isolated on a glutathione affinity column prior to cleavage with thrombin and elution of the free PH domain. This free GRP1-PH domain was further purified to homogeneity with a Sephadex G-75 gel filtration column. The mass of GRP1-PH was confirmed by matrix-assisted laser desorption/ionization time-of-flight mass spectroscopy (MALDI-TOF). Protein purity was determined by SDS−PAGE (*42*), and protein concentration was determined by both absorbance at 280 nm using the calculated extinction coefficient and the tyrosinate difference spectral method (*43*).

Preparation of Lipid Mixtures and Phospholipid Vesicles. Lipids were dissolved in chloroform/methanol/water (1/2/0.8) to give the desired lipid ratios, dried under vacuum at 45 °C until all solvents were removed, and then hydrated with buffer A (25 mM *N*-(2-hydroxyethyl)piperazine-*N*′-2-ethanesulfonic acid (HEPES), pH 7.4 with KOH, 140 mM KCl, and 15 mM NaCl, 1 mM $MgCl_2$) by rapid vortexing. Sonicated unilamellar phospholipid vesicles were prepared by sonication of the hydrated lipids to clarity with a Misonix XL2020 probe sonicator. Vesicles were prepared with a total lipid concentration of 3 mM having the following mole

percentages PE/PC/PS/PI/dPE/SM (42.75/19/19/9.5/5/4.75), PC/dPE/PI(3,4,5)P_3 (92/5/3), PC/PS/dPE/PI(3,4,5)P_3 (69/23/5/3), PE/PC/SM/dPE/PI(3,4,5)P_3 (59.1/26.3/6.6/5/3), PE/PC/PS/PI/dPE/SM/PI(3,4)P_2 (41.4/18.4/18.4/9.2/5/4.6/3), PE/PC/PS/PI/dPE/SM/PI(4,5)P_2 (41.4/18.4/18.4/9.2/5/4.6/3), PE/PC/PS/PI/dPE/SM/PI(3,4,5)P_3 (41.4/18.4/18.4/9.2/5/4.6/3). Following sonication, insoluble material was removed by centrifugation.

Equilibrium Fluorescence Experiments. Equilibrium fluorescence experiments were carried out on a Photon Technology International QM-2000-6SE fluorescence spectrometer at 25 °C in buffer A plus 10 mM dithiothreitol (DTT). The excitation and emission slit widths were 1 and 8 nm, respectively, for all measurements.

Measurement of IP_6 Binding to Free GRP1-PH Domain. The binding of IP_6 to GRP1-PH domain in the absence of lipids generates an increase in the intrinsic tryptophan fluorescence of the PH domain. To measure IP_6 binding to the free GRP1-PH domain, a concentrated IP_6 stock was titrated into a sample containing PH domain (0.8 μM) in buffer A plus 10 mM DTT. The intrinsic tryptophan fluorescence was monitored using excitation and emission wavelengths of $\lambda_{ex} = 284$ nm and $\lambda_{em} = 332$ nm. To control for the effects of the increasing ion concentration caused by the introduction of IP_6·12Na, a parallel control titration was carried out with free inorganic phosphate (Na_2HPO_4) in a separate cuvette containing free GRP1-PH domain such that the total phosphate concentration matched that of the IP_6 sample. The control was subtracted from the IP_6 titration data following correction for dilution. The resulting plot of intrinsic fluorescence as a function of IP_6 concentration was subject to nonlinear least-squares best-fit analysis to calculate the apparent dissociation constant for IP_6 ($K_D(IP_6)$), using eq 1, which describes binding to a single independent site:

$$F = \Delta F_{max}\left(\frac{x}{K_D + x}\right) \quad (1)$$

where ΔF_{max} represents the calculated maximal fluorescence change, x represents the total IP_6 concentration, and K_D represents the apparent macroscopic equilibrium dissociation constant for IP_6 binding. Finally, the best-fit ΔF_{max} value was normalized to unity to simplify graphical presentations.

Measurement of Protein-to-Membrane FRET. Analysis of protein-to-membrane FRET for GRP1-PH domain bound to membranes containing PIP lipids was carried out by titrating vesicles composed of PE/PC/PS/PI/dPE/SM, PE/PC/PS/PI/dPE/SM/PI(3,4)P_2, PE/PC/PS/PI/dPE/SM/PI(4,5)P_2, or PE/PC/PS/PI/dPE/SM/PI(3,4,5)P_3 (mole percentages above) with the PH domain according to methods previously developed for C2 domains (*44*, *45*). Briefly, sonicated lipids in buffer A were mixed with a solution containing GRP1-PH domain (1 μM) in buffer A plus 10 mM DTT, and the protein-to-membrane FRET was quantitated from the dPE emission (excitation and emission wavelengths were $\lambda_{ex} = 284$ nm and $\lambda_{em} = 522$ nm, respectively). In a separate sample, identical vesicles were added to buffer lacking protein to control for the increasing background emission arising from direct dPE excitation. Following subtraction of the background emission and correction for dilution, the FRET titration curve was best-fit with eq 1, and the best-fit ΔF_{max} value was normalized to unity.

FRET Competitive Binding Assay to Measure PIP Lipid Affinity and Specificity. Apparent equilibrium competitive inhibition constants ($K_I(IP_6)_{app}$) were determined by a competition assay in which membrane bound GRP1-PH domain is displaced from vesicles by the addition of the competitive inhibitor IP_6. Briefly, a concentrated IP_6 stock solution was titrated into the sample containing GRP1-PH domain (0.75 μM) and excess sonicated vesicles (101 μM total accessible lipid) in buffer A with 10 mM DTT. The competitive displacement of GRP1-PH domain from the membrane was monitored using protein-to-membrane FRET as described above. To control for the effects of the increasing ion concentration caused by the introduction of IP_6, a concentrated inorganic phosphate (Na_2HPO_4) solution was titrated in parallel into a separate but identical control sample to generate a total phosphate concentration equivalent to that of the IP_6 sample. The control titration data was subtracted from the IP_6 titration data following correction for dilution, and maximum fluorescence was normalized to one. Plots of protein-to-membrane FRET as a function of IP_6 concentration were subjected to nonlinear least-squares best-fit analysis using eq 2,

$$F = \Delta F_{max}\left(1 - \frac{x}{K_I(IP_6)_{app} + x}\right) + C \quad (2)$$

thereby yielding the apparent competitive inhibition constant for IP_6 ($K_I(IP_6)_{app}$). Finally, the best-fit offset C was subtracted from all data points, and the best-fit ΔF_{max} value was normalized to unity to simplify graphical presentations.

Stopped-Flow FRET Measurements of Association and Dissociation Kinetics. All kinetic experiments were done on an Applied Photophysics SX.17 stopped-flow fluorescence instrument at 25 °C in buffer A plus 10 mM DTT. The dead time of the instrument was 0.9 ± 0.1 ms; thus all data points prior to 1 ms were eliminated prior to quantitative analysis. To measure protein-to-membrane FRET in this instrument, the excitation wavelength and slit width settings on the excitation monochromator were 284 and 3 nm, respectively, while a 475 nm long-pass filter was used to select the detected wavelengths of emitted light.

To determine the observed rate constant for membrane association (k_{obs}) GRP1-PH domain (0.75 μM) was mixed by stopped-flow with vesicles (101 μM total accessible lipid). The resulting time course displayed an increasing level of protein-to-membrane FRET as noted above. The resulting time course was subjected to nonlinear least-squares best-fit analysis using either the single- or double-exponential function, eq 3 or 4, respectively:

$$F = \Delta F_{max}(1 - e^{-k_{obs}t}) + C \quad (3)$$

$$F = \Delta F_{max_1}(1 - e^{-k_{obs1}t}) + \Delta F_{max_2}(1 - e^{-k_{obs2}t}) + C \quad (4)$$

To simplify graphical presentations, the best-fit offset C was subtracted from all data points, and the best-fit ΔF_{max} (or, for the eq 4, $\Delta F_{max_1} + \Delta F_{max_2}$) value was normalized to unity. Finally, the observed rate constant was converted to the on-rate constant by division with the concentration of accessible target PIP lipid (equal to half the total target PIP lipid concentration since lipid exposed to the vesicle interior is inaccessible to protein).

To determine the rate constant for dissociation (k_{off}) of GRP1-PH from the membrane, the experiment began with the preformed binary complex of GRP1-PH domain (0.75 μM) and vesicles (101 μM total accessible lipid) in buffer A plus 10 mM DTT. At time zero, the binary complex was rapidly mixed with an equal volume of IP_6 (8.4 mM) in the same buffer. The resulting approach to equilibrium was monitored as a decrease in the protein-to-membrane FRET as the PH domain dissociated from the membrane. The resulting time course was subjected to nonlinear least-squares best-fit analysis using the single function eq 5:

$$F = \Delta F_{max}(e^{-k_{obs1}t}) + C \quad (5)$$

Finally, the best-fit offset C was subtracted from all data points, and the best-fit ΔF_{max} value was normalized to unity to simplify graphical presentations.

RESULTS

GRP1-PH Domain Expression and Purification. Human GRP1-PH domain was cloned as a GST fusion in *Escherichia coli* strain BL12D, overexpressed, and affinity purified. The free PH domain was generated by cleavage of the GST fusion with thrombin and subsequently purified to homogeneity by size-exclusion FPLC. The purity of the resulting GRP1-PH domain was determined by SDS−PAGE and found to exceed 90%. The mass of GRP1-PH domain was found to be 17 396 Da by MALDI-TOF mass spectroscopy, well within the range of error of the predicted mass (17 399 Da).

GRP1-PH Domain Lipid Specificity. The PIP lipid specificity of the isolated GRP1-PH domain was measured using a protein-to-membrane fluorescence resonance energy transfer (FRET) assay (*44*, *45*), which quantitates protein docking to synthetic membranes composed of well-defined mixtures of pure lipids. In the present application, the four intrinsic tryptophan residues of the PH domain (Trp270, -281, -285, and -371) serve as FRET donors and dansylated phosphatidylethanolamine (dPE), a fluorescent lipid incorporated into the membranes at small mole fraction, serves as the acceptor. FRET occurs only when the GRP1-PH domain is docked to the membrane surface, where all four tryptophans are expected to lie at distances (11−20 Å) from the headgroup region well within range required for efficient FRET ($R_o \approx$ 35 Å). The membranes utilized were sonicated unilamellar vesicles, which provided a stable bilayer structure similar to cellular membranes. To probe PIP lipid specificity, PH domain binding to three membrane-bound PIP lipids was compared: $PI(3,4,5)P_3$, the previously identified target of GRP1-PH domain (*30*, *33*), and two other important PIP signaling lipids, $PI(3,4)P_2$ and $PI(4,5)P_2$. Membranes lacking PIP lipids were also tested. The overall lipid composition of the membranes was a mixture designed to mimic the cytoplasmic leaflet of the plasma membrane (PE/PC/PS/PI/dPE/SM/PIP_x, 41.4/18.4/18.4/9.2/5/4.6/3 mol %).

Figure 1 illustrates the binding curves measured by titrating GRP1-PH domain into a suspension of each of the four membrane types while using protein-to-membrane FRET to monitor domain docking to the membrane surface. These binding curves indicate that GRP1-PH domain binds to $PI(3,4,5)P_3$-containing membranes with high affinity and to $PI(3,4)P_2$-containing membranes with substantially weaker affinity. No significant GRP1-PH domain binding is observed for $PI(4,5)P_2$-containing membranes nor for those lacking a PIP lipid. Such GRP1-PH domain titrations are useful for establishing relative affinities but not for accurate determination of affinities. This is especially true for the case of GRP1-PH domain binding to $PI(3,4,5)P_3$-containing membranes, where the protein concentration needed for the FRET assay significantly exceeds the K_D of the interaction (see below). Thus, a new experimental approach was developed to quantitatively determine the equilibrium affinity of PH domains for membrane-bound PIP lipids.

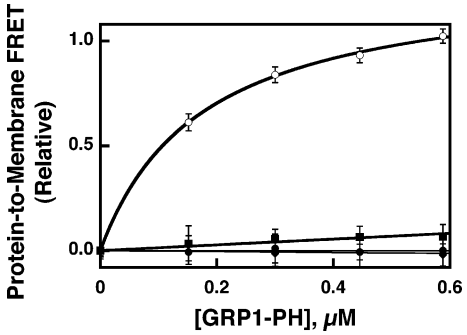

FIGURE 1: Equilibrium binding of GRP1-PH domain to synthetic lipid vesicles containing different PIP lipids. Sonicated lipid vesicles possessing the indicated PIP lipid exposed on their surfaces were titrated with isolated GRP1-PH domain (1 μM) at 25 °C. The docking of GRP1-PH domain to the vesicles was detected by protein-to-membrane FRET using intrinsic protein tryptophan residues as donors and membrane-bound dansyl-phosphatidylethanolamine lipids as acceptors (see Experimental Procedures). Vesicles were composed of PE/PC/PS/PI/dPE/SM/PIP_x (41.4/18.4/18.4/9.2/5/4.6/3 mol %) where the total accessible lipid and accessible PIP lipid concentrations were 59 and 1.8 μM, respectively, or PE/PC/PS/PI/dPE/SM (42.75/19/19/9.5/5/4.7/5 mol %) where the total accessible lipid was 59 μM, and the final buffer composition was 140 mM KCl, 15 mM NaCl, 1 mM $MgCl_2$, 10 mM DTT, 25 mM HEPES, pH 7.4. Individual samples contained $PI(3,4,5)P_3$ (○), $PI(3,4)P_2$ (■), $PI(4,5)P_2$ (◆), or no PIP lipid (●). Error bars represent the standard deviation of the mean for three replicate experiments.

FRET Competitive Binding Assay for Measuring High-Affinity PIP Lipid Binding: Approach. A new methodology was developed to quantitatively measure the equilibrium dissociation constant (K_D) for the high-affinity binding of a membrane docking protein to its target lipid in a membrane context. The method as applied to PH domains utilizes inositol-(1,2,3,4,5,6)-hexakisphosphate (IP_6) as a competitive inhibitor of PIP lipid binding, making use of the known ability of IP_6 to bind to a number of PH domains including the GRP1-PH domain (*30*−*32*, *34*, *46*). Briefly, the method first measures the affinity of the free PH domain for IP_6 in the absence of membranes. This step provides the equilibrium dissociation constant ($K_D(IP_6)$) for IP_6 binding to the free PH domain. Next, the IP_6 is used to competitively displace PH domain from its PIP lipid binding sites on target membranes. This step provides an apparent inhibition constant ($K_I(IP_6)_{app}$) for IP_6 that depends on the PIP lipid concentration and the background lipid composition, as well as the affinities of the PH domain for PIP lipid and for IP_6. Finally, the equilibrium dissociation constant ($K_D(PIP,X_Y)$) for PH domain binding to its PIP lipid target in a specific membrane context (X_Y) is calculated from the standard

Table 1: Lipid Composition of Sonicated Unilamellar Vesicles

lipid mixture	name	lipid mole ratio	lipid mol %
PC/PS/dPE/PI(3,4,5)P_3	S_A	22.5:7.5:1:1.5	69/23/5/3
PC/dPE/PI(3,4,5)P_3	S_N	30:1:1.5	92/5/3
PE/PC/PS/PI/dPE/SM/PI(3,4,5)P_3	P_A	13.5:6:6:3:1.5:1:1.5	41.4/18.4/18.4/9.2/5/4.6/3
PE/PC/SM/dPE/PI(3,4,5)P_3	P_N	19:9:2:1:1.5	59.1/26.3/6.6/5/3

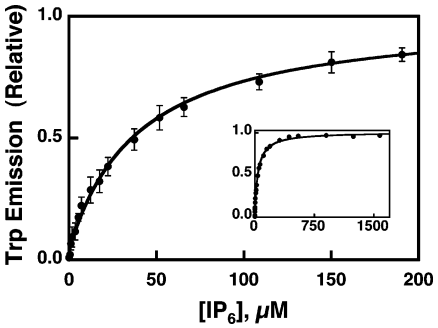

FIGURE 2: Equilibrium binding of IP_6 to isolated GRP1 PH domain in the absence of membranes. Free GRP1-PH domain (0.8 μM) was titrated at 25 °C with increasing concentrations of IP_6. Binding of IP_6 to the domain was monitored via the observed increase in intrinsic tryptophan fluorescence (see Experimental Procedures). The final buffer composition was 140 mM KCl, 15 mM NaCl, 1 mM $MgCl_2$, 1 mM DTT, 25 mM HEPES, pH 7.4). Error bars represent the standard deviation of the mean for four replicate experiments. The solid curve represents the nonlinear least-squares best fit for a homogeneous population of independent IP_6 binding sites (eq 1). Inset shows the same data over the full IP_6 concentration range used to calculate the binding constant.

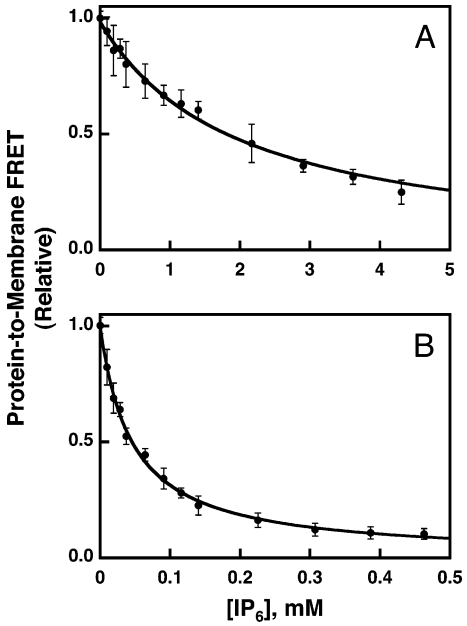

FIGURE 3: Use of FRET competitive binding assay to measure the equilibrium affinity of GRP1-PH domain for membrane-bound PIP lipids. A preformed complex between GRP1-PH domain (0.75 μM) and sonicated lipid vesicles containing the indicated PIP lipid (101 μM total accessible lipid; 3 μM accessible PIP lipid) was titrated at 25 °C with increasing concentrations of IP_6. The competitive displacement of GRP1-PH domain from the membrane surface was monitored as decreasing protein-to-membrane FRET (see Experimental Procedures). The final buffer composition was 140 mM KCl, 15 mM NaCl, 1 mM $MgCl_2$, 10 mM DTT, and 25 mM HEPES, pH 7.4. Membranes contained (A) PE/PC/PS/PI/dPE/SM/PI(3,4,5)-P_3 (41.4/18.4/18.4/9.2/5/4.6/3 mol %) or (B) PE/PC/PS/PI/dPE/SM/PI(3,4)P_2 membranes (41.4/18.4/18.4/9.2/5/4.6/3 mol %). Error bars represent the standard deviation of the mean for at least three replicate experiments. Solid curves represent nonlinear least-squares best fits for a homogeneous population of binding sites (eq 2), which yield the apparent IP_6 affinity, enabling calculation of the K_D for PH domain docking to membrane-bound PIP lipid (eq 6, Table 2).

competitive binding relationship:

$$K_I(IP_6)_{app} = K_D(IP_6)\left(1 + \frac{[PIP]_{free}}{K_D(PIP,X_Y)}\right) \qquad (6)$$

where $[PIP]_{free}$ is the free PIP concentration (2.6 $\pm$ 4 μM), which includes only that portion of the unbound PIP lipid population exposed on the outer surface of the vesicle where it is accessible to PH domain binding. For the PH domains examined thus far, including the GRP1-PH domain, this approach requires measurement of $K_D(IP_6)$ and $K_I(IP_6)_{app}$ values that fall in experimentally tractable ranges, rather than the experimentally less-accessible $K_D(PIP,X_Y)$ value. In the present study, four different background lipid compositions are utilized (X_Y corresponding to P_A, P_N, S_A, and S_N) as summarized in Table 1 and below.

Affinity of the Free GRP1-PH Domain for the Soluble Ligand IP6. Taking advantage of the increase in the intrinsic tryptophan fluorescence that occurs upon IP_6 binding to the GRP1-PH domain, an IP_6 binding curve was generated by titrating IP_6 into a solution of free PH domain in the absence of membranes while monitoring tryptophan emission. The resulting binding curve is shown in Figure 2. The data are well-approximated by a best-fit curve for a homogeneous population of independent IP_6 binding sites with a $K_D(IP_6)$ of 35 $\pm$ 2 μM. Since the apparent IP_6 affinity will decrease in the presence of PIP-lipid-containing membranes (eq 6), the measured $K_D(IP_6)$ is a lower limit on the apparent inhibition constant, $K_I(IP_6)_{app}$, for IP_6 disruption of PH domain−PIP lipid binding. Thus, the $K_I(IP_6)_{app}$ value will always exceed 35 μM, ensuring that the FRET competitive binding experiment will be straightforward since the IP_6 concentration range needed for the experiment will always significantly exceed the protein concentration in the fluorescence sample.

Quantitative Determination of GRP1-PH Domain PIP Specificity in a Physiological Membrane Context. The FRET competitive binding assay was used to quantitatively compare the affinity of GRP1-PH domain for target PIP lipids in the context of a lipid bilayer. The synthetic membranes used for this comparison were a mixture of pure PE/PC/PS/PI/dPE/SM/PIP_x, (mole percent 41.4/18.4/18.4/9.2/5/4.6/3) designed to mimic the physiological lipid background surrounding PIP lipids in the cytoplasmic leaflet of the plasma membrane (*47*). This mixture of background lipids is designated P_A (Table 1). Figure 3A presents the IP_6-triggered competitive displacement of GRP1-PH domain from P_A membranes containing 3 mol % PI(3,4,5)P_3, which yielded a $K_I(IP_6)_{app}$ of 2.0 $\pm$ 0.2 mM, which was in turn used to calculate a $K_D(PIP_3,P_A)$ of 50 $\pm$ 10 nM for the binding of

GRP1-PH domain to PI(3,4,5)P_3 in a physiological bilayer context (Figure 3A, eq 6). Similarly, competitive displacement from P_A membranes containing 3 mol % PI(3,4)P_2 yielded $K_I(IP_6)_{app}$ and K_D(PI(3,4)P_2,P_A) values of 46 ± 3 and 8 ± 3 μM, respectively (Figure 3B, eq 6). By contrast, the protein-to-membrane FRET signal obtained for P_A membranes containing 3 mol % PI(4,5)P_2 or P_A membranes lacking PIP lipids was too low for quantitation, confirming the results of the initial binding screen that indicated no detectable GRP1-PH domain binding to such membranes (Figure 1).

Overall, the findings indicate that the GRP1-PH domain possesses a 160-fold higher affinity for PI(3,4,5)P_3 than for PI(3,4)P_2 in a physiological bilayer context, while the unmeasurable affinity for PI(4,5)P_2 or for background lipids alone is at least 10^4-fold lower than the PI(3,4,5)P_3 affinity. In light of this clear specificity for PI(3,4,5)P_3, further studies of the GRP1-PH domain focused on the equilibrium and kinetic parameters for its docking to membranes containing PI(3,4,5)P_3, hereafter abbreviated PIP_3.

Determination of GRP1-PH Domain Equilibrium Dissociation Constants for PIP_3 in Different Membrane Contexts. To examine the effect of background lipids on GRP1-PH domain binding to PIP_3, the four different lipid mixtures summarized in Table 1 were utilized. The first mixture, PC/PS/dPE/PIP_3 (69/23/5/3 mol %), is based on the 3/1 PC/PS mixture often used as a simplified approximation of the cell membrane. Due to its simplified nature and to the fact that it contains the anionic lipid PS, this mixture is designated S_A. The second mixture is similar but replaces the anionic lipid PS with neutral PC yielding the mixture PC/dPE/PIP_3 (92/5/3 mol %), designated S_N. The third mixture is designed to mimic the physiological lipid composition of the plasma membrane inner leaflet and contains PE/PC/PS/PI/dPE/SM/PIP_3 (41.4/18.4/18.4/9.2/5/4.6/3 mol %), designated P_A. The final mixture is based on the latter physiological lipid mixture, but the anionic lipids PS and PI are removed to yield PE/PC/SM/dPE/PIP_3 (59.1/26.3/6.6/5/3 mol %), designated P_N.

Equilibrium dissociation constants ($K_D(PIP_3,X_Y)$) were measured for GRP1-PH domain binding to PIP_3 in each of these four membrane contexts using the FRET competitive binding assay. Figure 4 illustrates IP_6 titration curves for the displacement of GRP1-PH domain from membranes containing PIP_3 in the simple lipid background, both with and without the anionic lipid PS. The $K_I(IP_6)_{app}$ values measured for these PC/PS/dPE/PIP_3 (S_A) and PC/dPE/PIP_3 (S_N) membranes were 0.87 ± 0.07 and 0.17 ± 0.02 mM, respectively. These $K_I(IP_6)_{app}$ values were converted to equilibrium dissociation constants for GRP1-PH domain docking to PIP_3 in each simple background lipid context (eq 6), yielding a $K_D(PIP_3,S_A)$ value of 110 ± 20 nM and a $K_D(PIP_3,S_N)$ value of 700 ± 200 nM.

Figure 5 illustrates IP_6 titration curves for the displacement of GRP1-PH domain from membranes containing PIP_3 in the physiological lipid background, both with and without the anionic lipids PS and PI. The $K_I(IP_6)_{app}$ values measured for these PE/PC/PS/PI/dPE/SM/PIP_3 (P_A) and PE/PC/SM/dPE/PIP_3 (P_N) membranes were 2.0 ± 0.2 mM and 200 ± 20 μM, respectively. These $K_I(IP_6)_{app}$ values were converted to equilibrium dissociation constants for GRP1-PH domain docking to PIP_3 in each physiological background lipid context (eq 6), yielding a $K_D(PIP_3,P_A)$ value of 50 ± 10 nM and a $K_D(PIP_3,P_N)$ value of 600 ± 100 nM.

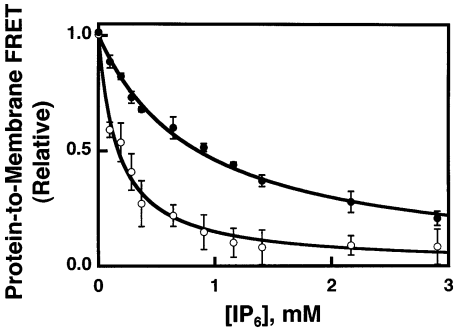

FIGURE 4: Use of FRET competitive binding assay to measure the equilibrium affinity of GRP1-PH domain for membrane-bound PIP_3 in a simple lipid mixture. A preformed complex between GRP1-PH domain (0.75 μM) and sonicated lipid vesicles containing PI(3,4,5)P_3 (101 μM total accessible lipid; 3 μM accessible PI(3,4,5)P_3) was titrated at 25 °C with increasing concentrations of IP_6. The competitive displacement of GRP1-PH domain from the membrane surface was monitored as decreasing protein-to-membrane FRET (see Experimental Procedures). The final buffer composition was 140 mM KCl, 15 mM NaCl, 1 mM $MgCl_2$, 10 mM DTT, 25 mM HEPES, pH 7.4, and membranes contained one of the two following lipid mixtures: PC/PS/dPE/PI(3,4,5)P_3 (69/23/5/3 mol %) (●) or PC/dPE/PI(3,4,5)P_3 (92/5/3 mol %) (○). Error bars represent the standard deviation of the mean for at least three replicate experiments. Solid curves represent nonlinear least-squares best fits for a homogeneous population of binding sites (eq 2), which yield the apparent IP_6 affinity, enabling calculation of the K_D for PH domain docking to membrane-bound PI(3,4,5)P_3 lipid (eq 6, Table 2).

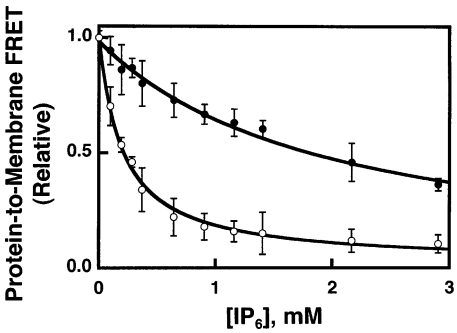

FIGURE 5: Use of FRET competitive binding assay to measure the equilibrium affinity of GRP1-PH domain for membrane-bound PIP_3 in a physiological lipid mixture. A preformed complex between GRP1-PH domain (0.75 μM) and sonicated lipid vesicles containing PI(3,4,5)P_3 (101 μM total accessible lipid; 3 μM accessible PI(3,4,5)P_3) was titrated at 25 °C with increasing concentrations of IP_6. The competitive displacement of GRP1-PH domain from the membrane surface was monitored as decreasing protein-to-membrane FRET (see Experimental Procedures). The final buffer composition was 140 mM KCl, 15 mM NaCl, 1 mM $MgCl_2$, 10 mM DTT, 25 mM HEPES, pH 7.4, and membranes contained one of the two following lipid mixtures: PE/PC/PS/PI/dPE/SM/PI(3,4,5)P_3 (41.4/18.4/18.4/9.2/5/4.6/3 mol %) (●) or PE/PC/SM/dPE/PI(3,4,5)P_3 (59.1/26.3/6.6/5/3 mol %) (○). Error bars represent the standard deviation of the mean for at least three replicate experiments. Solid curves represent nonlinear least-squares best fits for a homogeneous population of binding sites (eq 2), which yield the apparent IP_6 affinity, enabling calculation of the K_D for PH domain docking to membrane-bound PI(3,4,5)P_3 lipid (eq 6, Table 2).

Table 2 summarizes the equilibrium affinities for GRP1-PH domain docking to PIP_3 in each of the four background lipid contexts. Overall, the affinities of GRP1-PH domain for membrane-bound PIP_3 in the simple and physiological lipid mixtures are nearly the same, within 2-fold. When the

Table 2: Summary of Equilibrium and Kinetic Parameters for GRP1-PH Domain Docking to PIP_3 in Membranes

	equilibrium parameters[a]		kinetic parameters[a]		
lipid mixture	$K_I(IP_6)_{app}$ (mM)	$K_D(PIP_3)$[b] (nM)	k_{on} (s^{-1} μM^{-1})	k_{off} (s^{-1})	k_{off}/k_{on} (nM)
S_A	0.87 ± 0.07	110 ± 20	14 ± 2	1.3 ± 0.2	90 ± 20
S_N	0.17 ± 0.02	700 ± 200	2.5 ± 0.5	1.6 ± 0.2	600 ± 100
P_A	2.0 ± 0.2	50 ± 10	17 ± 3	1.1 ± 0.2	70 ± 20
P_N	0.20 ± 0.02	600 ± 100	1.4 ± 0.3	1.2 ± 0.2	900 ± 300

[a] Determined at 25 °C in samples containing 0.75 μM GRP1-PH domain and the indicated lipid mixture (see Table 1 for lipid compositions) in buffer containing 140 mM KCl, 15 mM NaCl, 1 mM $MgCl_2$, 10 mM DTT, and 25 mM HEPES, pH 7.4 with KOH. [b] Calculated from equilibrium parameters using eq 6.

anionic lipids PS and PI are removed, the GRP1-PH domain affinities for PIP_3 in the modified simple and physiological lipid mixtures are even more similar, but the loss of the anionic lipids decreases the affinity of GRP1-PH domain for its membrane-bound PIP_3 target by a factor of 6-fold or 12-fold in the simple and physiological lipid systems, respectively. It follows that background anionic lipids play a significant role in defining the observed affinity of the PH domain for PIP_3 in both membrane contexts.

Kinetic Analysis of GRP1-PH Domain Docking to PIP_3 Membranes. The kinetics of GRP1-PH domain membrane docking were studied to probe the kinetic basis of the affinity enhancement observed when the anionic lipids PS, or PS and PI, are present in PIP_3-containing membranes. In principle, such an affinity enhancement could arise from an increase in the on-rate constant (k_{on}) or a decrease in the off-rate constant (k_{off}) when the background anionic lipids are present. The time courses of GRP1-PH domain association and dissociation reactions were monitored by protein-to-membrane FRET in a stopped-flow fluorescence spectrometer. All conditions and concentrations utilized in these kinetic studies were identical to those of the equilibrium experiments to ensure that the kinetic and equilibrium results can be directly compared.

The association reaction was triggered by rapid mixing (<1 ms) of a membrane suspension with a solution of GRP1-PH domain while monitoring the increase in protein-to-membrane FRET as the protein docked to the membrane. An excess of available PIP_3, together with the high affinity of the PH domain for its target, ensured that the vast majority of PH domain became membrane bound as equilibrium was achieved. As a result, the contribution of dissociation kinetics to the observed approach to equilibrium was negligible. The time course of GRP1-PH domain docking to simple PC/PS/dPE/PIP_3 membranes (Table 1) is shown in Figure 6A. Nonlinear least-squares best-fit analysis revealed that a double-exponential function was required to adequately fit the data, yielding the primary observed rate constant, $k_{obs}(S_A) = 38 \pm 1\ s^{-1}$, corresponding to the majority of the association curve amplitude. This observed rate constant was then divided by the concentration of accessible PIP_3 to yield the on-rate constant, $k_{on}(S_A) = 14 \pm 1\ s^{-1}\ \mu M^{-1}$. When PS was removed from the simple membranes, the time course of GRP1-PH domain docking was slowed significantly (compare Figure 6A,B). The resulting kinetic data was adequately fit by a single-exponential function, yielding the observed rate constant, $k_{obs}(S_N) = 7 \pm 1\ s^{-1}$. This observed rate constant was subsequently corrected for the concentration of accessible PIP_3 to yield the on-rate constant, $k_{on}(S_N) = 2.5 \pm 0.5\ s^{-1}\ \mu M^{-1}$. Thus, the removal of the anionic lipid PS from the simple membranes yields a 6-fold decrease in the magnitude of the on-rate constant (Table 2).

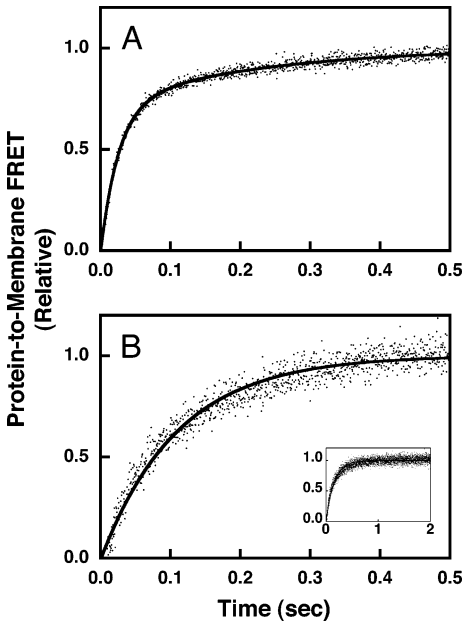

FIGURE 6: Association kinetics of GRP1-PH domain docking to membrane-bound PIP_3 in a simple lipid mixture. The association reaction was triggered by rapid mixing of GRP1-PH domain with sonicated lipid vesicles containing PI(3,4,5)P_3 at 25 °C in a stopped-flow spectrofluorimeter while monitoring the increasing protein-to-membrane FRET (see Experimental Procedures). The GRP1-PH domain and lipid concentrations following mixing were equivalent to those used in the equilibrium experiments (0.75 μM GRP1-PH domain; 101 μM total lipid accessible; 3 μM PI(3,4,5)P_3 accessible). The buffer contained 140 mM KCl, 15 mM NaCl, 1 mM $MgCl_2$, 1 mM DTT, and 25 mM HEPES, pH 7.4, and the membranes were composed of (A) PC/PS/dPE/PI(3,4,5)P_3 (69/23/5/3 mol %) or (B) PC/dPE/PI(3,4,5)P_3 (92/5/3 mol %). Data points represent the average values from at least six separate replicate timecourses. The solid curves represent the best fit to (A) a double-exponential equation or (B) a single-exponential equation (eq 3 or 4, respectively). Panel B inset shows the same data over the full time course used to determine k_{on}.

The dissociation reaction was triggered by stopped-flow mixing (<1 ms) a suspension of GRP1-PH domain bound to PIP_3-containing membranes with a solution of the competitive inhibitor IP_6. In the presence of saturating IP_6, as the domain dissociated from the membrane, it was rapidly occupied by the inhibitor, thereby effectively making membrane dissociation an irreversible reaction. The dissociation time course was monitored by following the decreasing protein-to-membrane FRET as the protein left the membrane surface, as illustrated in Figure 7. For simple membranes containing and lacking PS, the resulting kinetic data was adequately fit by a single-exponential function, yielding the off-rate constants $k_{off}(S_A) = 1.3 \pm 0.2$ and $k_{off}(S_N) = 1.6 \pm 0.2\ s^{-1}$. Thus, the off-rate constants measured for simple membranes containing and lacking the anionic lipid PS were very similar (Table 2).

Analogous kinetic measurements of association and dissociation time courses were carried out for physiological PE/PC/PS/PI/SM/dPE/PIP_3 membranes (Table 1) containing and lacking the anionic lipids PS and PI. For physiological

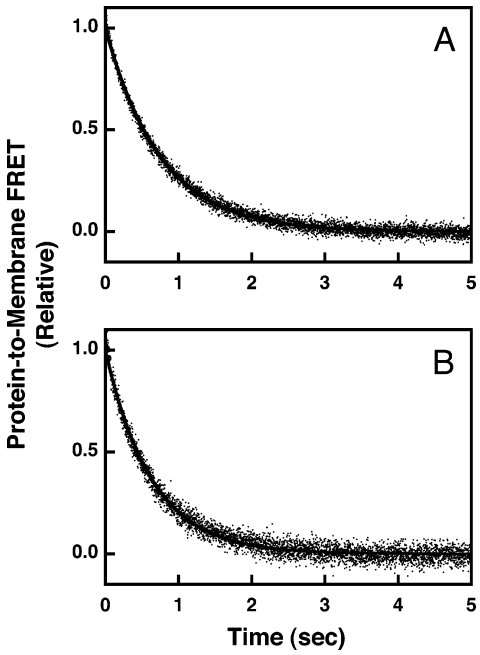

FIGURE 7: Dissociation kinetics of GRP1-PH domain docked to membrane-bound PIP_3 in a simple lipid mixture. The dissociation reaction was triggered by rapid mixing of IP_6 with GRP1-PH domain bound to $PI(3,4,5)P_3$ on vesicles in a stopped-flow fluorimeter at 25 °C. The resulting dissociation of GRP1-PH domain from the vesicles was monitored by protein-to-membrane FRET (see Experimental Procedures). The GRP1-PH domain and lipid concentrations following mixing were equivalent to those used in the equilibrium experiments (0.75 μM GRP1-PH; 101 μM total lipid accessible; 3 μM $PI(3,4,5)P_3$ accessible). The buffer contained 140 mM KCl, 15 mM NaCl, 1 mM $MgCl_2$, 10 mM DTT, and 25 mM HEPES, pH 7.4, and the membranes were composed of (A) PC/PS/dPE/$PI(3,4,5)P_3$ (69/23/5/3 mol %) or (B) PC/dPE/$PI(3,4,5)P_3$ (92/5/3 mol %). Data points represent the average values from at least six separate replicate time courses. The solid curves represent the best fits to a single-exponential equation (eq 5).

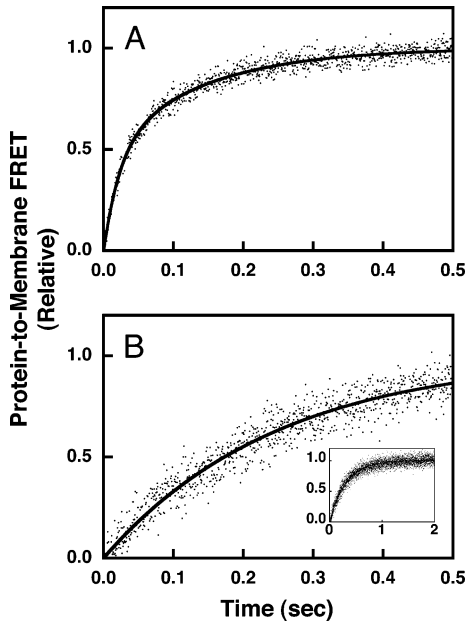

FIGURE 8: Association kinetics of GRP1-PH domain docking to membrane-bound PIP_3 in a physiological lipid mixture. The association reaction was triggered by rapid mixing of GRP1-PH domain with sonicated lipid vesicles containing $PI(3,4,5)P_3$ at 25 °C in a stopped-flow spectrofluorimeter while monitoring the increasing protein-to-membrane FRET (see Experimental Procedures). The GRP1-PH domain and lipid concentrations following mixing were equivalent to those used in the equilibrium experiments (0.75 μM GRP1-PH domain: 101 μM total lipid accessible; 3 μM $PI(3,4,5)P_3$ accessible). The buffer contained 140 mM KCl, 15 mM NaCl, 1 mM $MgCl_2$, 10 mM DTT, and 25 mM HEPES, pH 7.4, and the membranes were composed of (A) PE/PC/PS/PI/dPE/SM/$PI(3,4,5)P_3$ (41.4/18.4/18.4/9.2/5/4.6/3 mol %) or (B) PE/PC/SM/dPE/$PI(3,4,5)P_3$ (59.1/26.3/6.6/5/3 mol %). Data points represent the average values from at least six separate replicate time courses. The solid curves represent the best fit to (A) a double-exponential equation or (B) a single-exponential equation (eq 3 or 4, respectively). Panel B inset shows the same data over the full time course used to determine k_{on}.

membranes in the presence of anionic lipids, the time course of the association reaction required a double-exponential function to adequately fit the data as illustrated in Figure 8A, yielding the primary observed rate constant, $k_{obs}(P_A) = 44 \pm 2\ s^{-1}$, corresponding to the majority of the association curve amplitude. Division of the observed rate constant by the concentration of accessible PIP_3 yielded the on-rate constant, $k_{on}(P_A) = 17 \pm 3\ s^{-1}\ \mu M^{-1}$, for docking to physiological membranes. When the anionic lipids PS and PI were removed from the physiological lipid mixture, a single-exponential function was adequate to fit the association reaction (Figure 8B), yielding the observed rate constant, $k_{obs}(P_N) = 3.5 \pm 0.5\ s^{-1}$, and, following correction for the accessible PIP_3 concentration, the on-rate constant, $k_{on}(P_N) = 1.4 \pm 0.3\ s^{-1}\ \mu M^{-1}$. Thus, removal of the anionic lipids PS and PI from the lipid mixture slows the rate of GRP1-PH domain docking to PIP_3 in physiological membranes by a factor of 12.

The time courses for dissociation from physiological membranes containing and lacking the anionic lipics PS and PI were adequately fit by a single-exponential function, as illustrated in Figure 9. The resulting off-rate constants were $k_{off}(P_A) = 1.1 \pm 0.2$ and $k_{off}(P_N) = 1.2 \pm 0.2\ s^{-1}$ for physiological membranes containing and lacking the anionic lipids PS and PI, respectively. Thus, as in the case of simple membranes, the dissociation kinetics were not significantly altered by removal of background anionic lipids.

Overall, for both the simple lipid mixture and the more complex physiological lipid mixture, the presence of background anionic lipids significantly speeds the rate of binding of GRP1-PH domain to membrane-bound PIP_3 but has little or no effect on the rate of dissociation. The 6-fold and 12-fold faster association rates fully explain the 6-fold and 12-fold higher affinities observed for equilibrium GRP1-PH domain binding to simple and physiological membranes that contain the full complement of anionic lipids, respectively. Notably, equilibrium dissociation constants calculated from the kinetic data ($K_D = k_{off}/k_{on}$) are in good agreement with the experimental dissociation constants measured by the FRET competitive binding assay (Table 2). This self-consistency provides strong evidence that the kinetic analysis accurately depicts the rates of the microscopic processes occurring during equilibrium binding. Moreover, the good agreement supports the use of the fast, major-amplitude component from the double-exponential fits to calculate the on-rate constants for membranes containing anionic lipids. The minor-amplitude component of these fits is 6-fold to 8-fold slower than the major component, and the simplest explanation for the slow component is that PH domain docking triggers a slow rearrangement of lipids involving

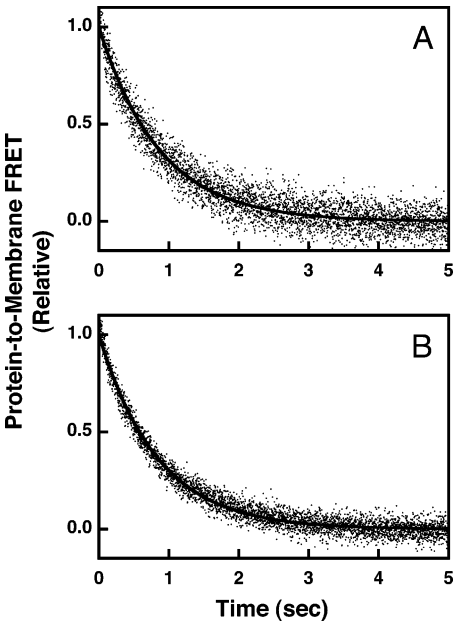

FIGURE 9: Dissociation kinetics of GRP1-PH domain docked to membrane-bound PIP_3 in a physiological lipid mixture. The dissociation reaction was triggered by rapid mixing of IP_6 with GRP1-PH domain bound to $PI(3,4,5)P_3$ on vesicles in a stopped-flow fluorimeter at 25 °C. The resulting dissociation of GRP1-PH domain from the vesicles was monitored by protein-to-membrane FRET (see Experimental Procedures). The GRP1-PH domain and lipid concentrations following mixing were equivalent to those used in the equilibrium experiments (0.75 μM GRP1-PH domain; 101 μM total lipid accessible; 3 μM $PI(3,4,5)P_3$ accessible). The buffer contained 140 mM KCl, 15 mM NaCl, 1 mM $MgCl_2$, 10 mM DTT, and 25 mM HEPES, pH 7.4, and the membranes were composed of (A) PE/PC/PS/PI/dPE/SM/$PI(3,4,5)P_3$ (41.4/18.4/18.4/9.2/5/4.6/3 mol %) or (B) PE/PC/SM/dPE/$PI(3,4,5)P_3$ (59.1/26.3/6.6/5/3 mol %). Data points represent the average values from at least six separate replicate time courses. The solid curves represent the best fits to a single-exponential equation (eq 5).

PS and PI, since no slow component is observed in the association reaction when membranes lack one or both of these background anionic lipids. Such redistribution of lipids has previously been observed following the binding of certain proteins to membrane surfaces (*48*, *49*). Also notable is the observation that dissociation of the GRP1-PH domain from all four types of membrane yields a single-exponential time course and a nearly identical off-rate constant ($\sim 1\ s^{-1}$), independent of whether background anionic lipids are present. It follows that once the PH domain is stably bound to its target PIP_3 lipid, its dissociation from the membrane is relatively insensitive to the anionic lipid composition of the surrounding lipid mixture.

DISCUSSION

The present study uses a protein-to-membrane FRET assay, previously developed for C2 domains (*44*, *45*), to monitor PH domain docking to target lipids in synthetic bilayers of controlled composition. The advantages of this assay include high sensitivity and precision, use of minimal quantities of lipids and proteins, and avoidance of membrane stresses due to loading of vesicles with the nonphysiological solutes used in pelleting methods. Furthermore, a novel extension of this protein-to-membrane FRET approach has enabled the development of a competitive binding assay that accurately measures very high PH domain affinities for membrane-bound target lipids that are difficult to quantitate by standard methods.

Equilibrium binding measurements using this FRET competitive binding assay confirm predictions based on soluble analogue studies that the GRP1-PH domain would be specific for membrane-bound $PI(3,4,5)P_3$ and also would exhibit weak binding to membrane-bound $PI(3,4)P_2$ but not to $PI(4,5)P_2$ (*27*, *30*, *33*, *50*). The present results reveal that the GRP1-PH domain binds to membrane-bound $PI(3,4)P_2$ and $PI(4,5)P_2$ with 160-fold lower and $>10^4$-fold lower affinities, respectively, than $PI(3,4,5)P_3$ in the same lipid background. Thus, the GRP1-PH domain exhibits at least a 2-log preference for target lipid $PI(3,4,5)P_3$ relative to other membrane-bound PIP lipids.

The present work also examines the docking of GRP1-PH domain to $PI(3,4,5)P_3$ (hereafter termed PIP_3) in different background lipid mixtures, thereby analyzing the effect of bilayer context on the docking equilibrium and kinetics. The results indicate that the PH domain docks with similar (within 2-fold) affinities to PIP_3 in either a simplified lipid mixture (PC/PS/dPE/PIP_3, 69/23/5/3 mol %) or a physiological lipid mixture designed to mimic the lipid composition of the plasma membrane inner leaflet (PE/PC/PS/PI/dPE/SM/PIP_3, 41.4/18.4/18.4/9.2/5/4.6/3 mol %). Removal of the anionic lipid PS from the simple lipid mixture reduces the GRP1-PH domain affinity for membrane-bound PIP_3 6-fold. Similarly, removal of anionic lipids PS and PI from the physiological lipid mixture reduces the PH domain affinity for membrane-bound PIP_3 12-fold. Thus, the affinity of GRP1-PH domain for its target PIP_3 is dependent on the composition of the background lipids, providing evidence for direct or indirect interactions between the PH domain and nontarget lipid components of the membrane surface.

To probe the mechanism by which anionic background lipids increase the PH domain affinity for membrane-bound PIP_3, the effects of these lipids on association and dissociation kinetics have been measured. Notably, the equilibrium and kinetic data are self-consistent (as indicated by $K_D = k_{off}/k_{on}$, see Table 2), providing strong evidence for the accuracy of both types of data. The on-rate for the association of GRP1-PH domain with membrane-bound PIP_3 in the simple lipid mixture is 6-fold faster when the mixture contains the anionic lipid PS, while the off-rate for PH domain dissociation from these membranes is independent, within error, of whether the mixture contains or lacks PS. Similarly, the on-rate for association of GRP1-PH domain with membrane-bound PIP_3 in the physiological lipid mixture is 12-fold faster when the mixture contains the anionic lipids PS and PI, while the off-rate for PH domain dissociation from the physiological membranes is independent of whether the mixture contains or lacks these anionic lipids. Thus, the PIP_3 affinity enhancement provided by the presence of background anionic lipids arises entirely from a faster on-rate for docking to the membrane-bound PIP_3 rather than from a slower membrane dissociation. Such enhancement of the on-rate by background anionic lipids has important implications for the mechanism used by the GRP1-PH domain to find its rare target lipid.

During a cellular signaling event, PIP_3 is generated as a rare lipid component in the cytoplasmic leaflet of the plasma membrane. Most of this rare target lipid is generated by the class I phosphoinositide 3-kinases (PI3Ks) through the

phosphorylation of the precursor lipid $PI(4,5)P_2$ to yield PIP_3 (*5*). Estimates of the cellular quantities of $PI(4,5)P_2$ and PIP_3 vary widely, but the available information suggests that the total cytoplasmic concentration of PIP_3 ranges from approximately 2 nM in a resting cell to a peak cytoplasmic concentration of 200 nM in a stimulated cell. (These values assume that (i) $PI(4,5)P_2$ represents 2% of the lipids in the cytoplasmic leaflet of the plasma membane, (ii) the resting and peak levels of PIP_3 are 0.01% and 1% of total $PI(4,5)P_2$ in the cytoplasmic leaflet, respectively, (iii) the total number of lipids in the cytoplasmic leaflet is 5×10^8, and (iv) the cytoplasmic volume is 1 pL (*5*, *25*, *48*, *51*, *52*). Significantly, the K_D of 50 nM measured herein for the binding of GRP1-PH domain to membrane-bound PIP_3 in a physiological lipid context is perfectly tuned to act as a recruitment switch in these cytoplasmic PIP_3 concentrations. Thus, as the cytoplasmic PIP_3 concentration increases from approximately 2 nM to a peak value of 200 nM during a signaling event, the affinity of the PH domain for the plasma membrane would increase dramatically as expected for a targeting motif.

The peak signaling concentration of PIP_3 can further be used to estimate the time scale of GRP1-PH domain docking to membrane-bound PIP_3 in a cellular context. The present data (Figure 8) illustrate the time scale of the docking reaction for GRP1-PH domain docking to membrane-bound PIP_3 in a physiological lipid mixture; however, the total accessible PIP_3 concentration is 13-fold higher than the 200 nM peak concentration estimated for a cellular signaling event. It follows that in the cellular context, the docking time course could be slowed at least 13-fold by the lower PIP_3 concentration. In this scenario, the docking reaction would take at least 2 s to reach completion (obtained by 13-fold slowing of the time course in Figure 8A). If anionic lipids were not present, the docking reaction would be further slowed and would take at least 20 s to reach completion (obtained by 13-fold slowing of the time course in Figure 8B). Given that cellular PIP_3 signals can be generated within 10 s and can decay within 30 s in fast pathways such as chemotaxis (*53*, *54*), the interaction of GRP1-PH domain with anionic lipids is likely to play a physiologically relevant role in allowing PH domain recruitment to rapidly track changing PIP_3 levels at the plasma membrane surface. Overall, the available evidence suggests that the rate enhancement provided by interactions with background anionic lipids plays a physiologically relevant role in speeding the docking and activation kinetics of GRP1 in vivo, especially in pathways that generate rapid signals. Moreover, such rate enhancement may be even more important in cells where large numbers of other proteins bind PIP_3, thereby effectively lowering the concentration of free signaling lipid available for GRP1 docking.

Figure 10 presents a model that explains the effects of background anionic lipids on the on-rate constant (k_{on}) and the equilibrium dissociation constant (K_D) for GRP1-PH domain docking to membrane-bound PIP_3. When the PH domain approaches the cytoplasmic leaflet of the plasma membrane, the highly basic PIP docking face observed on the GRP1-PH domain and other PH domains (*15*, *17*, *55*) is proposed to interact weakly with anionic lipids on the membrane surface (predominantly PS and PI). For GRP1-PH domain, the affinity of this nonspecific electrostatic interaction is too low to measure; thus the interaction does not drive a significant fraction of the PH domain population onto the membrane. Such a weak interaction ensures that there is little or no premature membrane docking in the absence of a PIP_3 signal. However, the weak interaction increases the residence time of the PH domain in the vicinity of the membrane and thereby also increases the rate of collisions of the PH domain with the membrane surface. Moreover, electrostatic steering toward the anionic back-

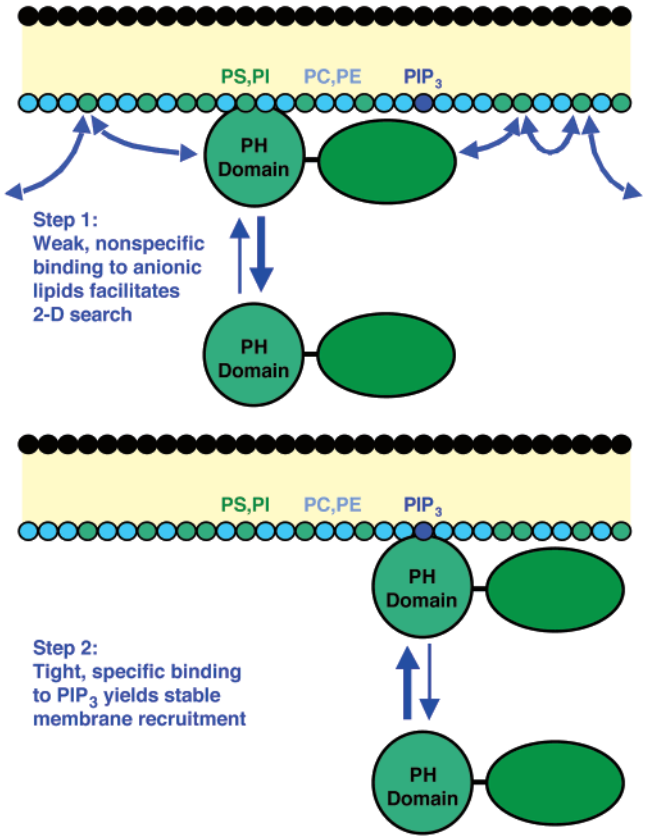

FIGURE 10: Model of the search mechanism used by GRP1-PH domain to find the rare target lipid PIP3. Shown is a schematic plasma membrane consisting of a core hydrocarbon region (yellow), the headgroups of the outer leaflet (black) and the headgroups of the cytoplasmic inner leaflet color coded according to chemical identity (cyan for neutral headgroups, green for the anionic lipids PS and PI, and blue for $PI(3,4,5)P_3$). Also shown is the full-length GRP1 protein with its distinct PH and GEF (guanine-nucleotide exchange factor) domains. Panel A depicts step 1: The PH domain of cytosolic GRP1 forms transient weak electrostatic interactions with the abundant background anionic lipids PS and PI. The nonspecific electrostatic interactions with PS and PI are not sufficient to generate stable docking of GRP1 to the membrane but are sufficient to significantly increase the residency time of the protein at or near the membrane. This increased residency time near the membrane facilitates electrostatic steering, as well as a short-range two-dimensional search across the membrane surface for the rare target PIP_3. Yet the membrane association is transient, and the bold arrow emphasizes that the equilibrium favors the free cytosolic state of the protein, while the curved arrows indicate that the short intervals of the two-dimensional search are frequently interrupted by dissociation events. Panel B depicts step 2: Once its target lipid has been found, the PH domain of GRP1 binds specifically and with high affinity to PIP_3 resulting in stable membrane docking. The bold arrow emphasizes that the equilibrium favors the membrane-bound state of the protein. The dissociation event is dominated by the interaction with PIP_3 and perhaps additional hydrophobic interactions with the surrounding membrane, but electrostatic interactions with the surrounding membrane appear to be minor by comparison since background anionic lipids have little effect on the dissociation kinetics (see text).

ground lipids (*56*, *57*) helps rotate the PH domain into the correct orientation for membrane docking. These factors increase the probability that the PH domain will hop along the membrane surface until it finds a PIP_3 target lipid and docks. In short, the weak electrostatic interaction with anionic lipids increases the likelihood that the PH domain will execute a transient, stochastic two-dimensional search of the membrane surface before it returns to the bulk population in the cytosol, thereby enhancing the efficiency of the search process at least 10-fold when anionic lipids are present. Once the PH domain is docked to PIP_3 its dissociation rate is determined by the high-affinity interaction with the target lipid and perhaps additional hydrophobic interactions with the surrounding membrane (*17*, *58*, *59*), but electrostatic interactions with the surrounding membrane appear to be minor by comparison, thus the dissociation rate is independent of background anionic lipids.

In a cellular context, the enhancement of on-rate and equilibrium affinity provided by weak interactions with anionic lipids could be even greater than observed in the present study, since the PIP_3 densities achieved during peak cellular signals is at least 10-fold lower than that used herein. Preliminary studies indicate that the enhancement factor increases as the PIP_3 density decreases (Corbin and Falke, unpublished), presumably because search efficiency becomes more important as one moves from high to low PIP_3 densities. Other PH domains may share this search mechanism; for example, the PH domains from the GRP1 homologues ARNO and PLCδ1 have both been observed to bind weakly to the anionic background lipid PS in addition to their target PIP lipids (*28*, *36*). Moreover, PLCδ1-PH exhibits a 10-fold greater affinity for $PI(4,5)P_2$ membranes containing PS and PI than for membranes lacking background anionic lipids (*36*, *38*). While the mechanistic basis for the affinity enhancement due to PS and PI has not been experimentally investigated, molecular modeling studies suggest that nonspecific electrostatic interactions could contribute to the membrane association of PLCδ1-PH (*55*).

The present findings provide the first direct evidence that a PH domain uses a two-dimensional search mechanism to more rapidly find its rare target lipid. Evidence that a different type of two-dimensional search mechanism is used by protein kinase C βII has been presented (*60*, *61*). During the membrane targeting of this protein, the Ca^{2+}-activated C2 domain first docks to the anionic lipid PS on the plasma membrane surface, thereby effectively tethering the protein to the plasma membrane, while its C1 domain searches for the more rare target lipid diacylglycerol. In this example, however, both membrane recruitment and targeting are accomplished in the first binding step, and the binding interactions with common and rare lipids are generated by different domains. By contrast, for the GRP1-PH domain, the initial nonspecific binding to anionic lipids is too weak to accomplish membrane targeting, and the binding surfaces for common and rare lipids are combined in the same domain. Further studies are needed to determine the generality of two-dimensional searching in PH domain targeting.

Finally, comparison of the K_D values for GRP1-PH domain binding to soluble PIP_3 analogues and to membrane-bound PIP_3 reveals an important difference. The published K_D values for soluble analogues range from 50 nM for a soluble dioctanoyl form of PIP_3 (*27*) to 30 nM for $I(1,3,4,5)P_4$ (*30*, *31*). By contrast, the K_D value measured herein for PIP_3 in neutral membranes lacking other anionic lipids is 700 nM. (The use of membranes lacking anionic lipids is most appropriate for the purposes of this comparison since anionic lipids would enable a target search mechanism not present in solution). It follows that the observed affinity for neutral membrane-bound PIP_3 is an order of magnitude lower than for the soluble analogues. Similarly, previous studies have shown that the PLCδ1-PH domain binds $PI(4,5)P_2$ incorporated into neutral membranes an order of magnitude more weakly than soluble analogues of $PI(4,5)P_2$ (*36*). There are two simple explanations for these observations. First, the GRP1- and PLCδ1-PH domains could have thermodynamically unfavorable interactions with the neutral background lipids surrounding their target lipids, which, in the broader context of the biological membrane, could play an important role in tuning the affinity of each PH domain as appropriate for cellular signal amplitudes. Alternatively, if the target lipid binding reaction is diffusion-limited, the lower affinity for membrane-bound target could have a purely kinetic explanation. In this scenario, the membrane-bound target lipid on the surface of a nearly stationary vesicle would collide approximately 10-fold more slowly with the PH domain than a rapidly diffusing, soluble target analogue. As a result, the membrane-bound target lipid would yield a significantly slower on-rate and higher K_D value than a soluble headgroup analogue. Further studies are needed to resolve the thermodynamic and kinetic hypotheses for the affinity loss observed when PH domain target lipids are incorporated into neutral membranes.

In either case, the thermodynamic and kinetic hypotheses both emphasize that it is simply a coincidence that GRP1-PH domain exhibits similar affinities for soluble PIP_3 analogues (K_D of 30−50 nM) (*27*, *30*, *31*) and for PIP_3 in physiological membranes containing the anionic lipids PS and PI (K_D of 50 nM) (measured herein). Such coincident affinities arise from the on-rate enhancement provided by interactions between the PH domain and background anionic lipids, which restores the overall affinity for neutral membrane-bound target lipid back to the level observed for soluble analogues. It follows that the on-rate enhancement generated by nonspecific interactions with ionic lipids plays an essential role in ensuring not only rapid binding to target lipid but also the carefully optimized target lipid affinity needed for physiological signaling processes.

REFERENCES

1. Yu, J. W., Mendrola, J. M., Audhya, A., Singh, S., Keleti, D., DeWald, D. B., Murray, D., Emr, S. D., and Lemmon, M. A. (2004) Genome-wide analysis of membrane targeting by S. cerevisiae pleckstrin homology domains, *Mol. Cell 13*, 677−88.
2. Czech, M. P. (2003) Dynamics of phosphoinositides in membrane retrieval and insertion, *Annu. Rev. Physiol. 65*, 791−815.
3. Luo, J., Manning, B. D., and Cantley, L. C. (2003) Targeting the PI3K-Akt pathway in human cancer: rationale and promise, *Cancer Cell 4*, 257−62.
4. Hurley, J. H., and Meyer, T. (2001) Subcellular targeting by membrane lipids, *Curr. Opin. Cell Biol. 13*, 146−52.
5. Vanhaesebroeck, B., Leevers, S. J., Ahmadi, K., Timms, J., Katso, R., Driscoll, P. C., Woscholski, R., Parker, P. J., and Waterfield, M. D. (2001) Synthesis and function of 3-phosphorylated inositol lipids, *Annu. Rev. Biochem. 70*, 535−602.
6. Czech, M. P. (2000) PIP2 and PIP3: complex roles at the cell surface, *Cell 100*, 603−6.

7. Letunic, I., Copley, R. R., Schmidt, S., Ciccarelli, F. D., Doerks, T., Schultz, J., Ponting, C. P., and Bork, P. (2004) SMART 4.0: towards genomic data integration, *Nucleic Acids Res. 32* (Database issue), D142−4.
8. Cozier, G. E., Carlton, J., Bouyoucef, D., and Cullen, P. J. (2004) Membrane targeting by pleckstrin homology domains, *Curr. Top Microbiol. Immunol. 282*, 49−88.
9. Lemmon, M. A. (2003) Phosphoinositide recognition domains, *Traffic 4*, 201−13.
10. Lemmon, M. A., and Ferguson, K. M. (2000) Signal-dependent membrane targeting by pleckstrin homology (PH) domains, *Biochem. J. 350* (Part 1), 1−18.
11. Hurley, J. H., and Misra, S. (2000) Signaling and subcellular targeting by membrane-binding domains, *Annu. Rev. Biophys. Biomol. Struct. 29*, 49−79.
12. Fruman, D. A., Rameh, L. E., and Cantley, L. C. (1999) Phosphoinositide binding domains: embracing 3-phosphate, *Cell 97*, 817−20.
13. Baraldi, E., Carugo, K. D., Hyvonen, M., Surdo, P. L., Riley, A. M., Potter, B. V., O'Brien, R., Ladbury, J. E., and Saraste, M. (1999) Structure of the PH domain from Bruton's tyrosine kinase in complex with inositol 1,3,4,5-tetrakisphosphate, *Struct. Fold Des. 7*, 449−60.
14. Ferguson, K. M., Lemmon, M. A., Schlessinger, J., and Sigler, P. B. (1995) Structure of the high affinity complex of inositol trisphosphate with a phospholipase C pleckstrin homology domain, *Cell 83*, 1037−46.
15. Ferguson, K. M., Kavran, J. M., Sankaran, V. G., Fournier, E., Isakoff, S. J., Skolnik, E. Y., and Lemmon, M. A. (2000) Structural basis for discrimination of 3-phosphoinositides by pleckstrin homology domains, *Mol. Cell 6*, 373−84.
16. Hyvonen, M., Macias, M. J., Nilges, M., Oschkinat, H., Saraste, M., and Wilmanns, M. (1995) Structure of the binding site for inositol phosphates in a PH domain, *EMBO J. 14*, 4676−85.
17. Lietzke, S. E., Bose, S., Cronin, T., Klarlund, J., Chawla, A., Czech, M. P., and Lambright, D. G. (2000) Structural basis of 3-phosphoinositide recognition by pleckstrin homology domains, *Mol. Cell 6*, 385−94.
18. Thomas, C. C., Deak, M., Alessi, D. R., and van Aalten, D. M. (2002) High-resolution structure of the pleckstrin homology domain of protein kinase b/akt bound to phosphatidylinositol (3,4,5)-trisphosphate, *Curr. Biol. 12*, 1256−62.
19. Cantley, L. C. (2002) The phosphoinositide 3-kinase pathway, *Science 296*, 1655−7.
20. Rameh, L. E., and Cantley, L. C. (1999) The role of phosphoinositide 3-kinase lipid products in cell function, *J. Biol. Chem. 274*, 8347−50.
21. Sadhu, C., Masinovsky, B., Dick, K., Sowell, C. G., and Staunton, D. E. (2003) Essential role of phosphoinositide 3-kinase delta in neutrophil directional movement, *J. Immunol. 170*, 2647−54.
22. Servant, G., Weiner, O. D., Herzmark, P., Balla, T., Sedat, J. W., and Bourne, H. R. (2000) Polarization of chemoattractant receptor signaling during neutrophil chemotaxis, *Science 287*, 1037−40.
23. Devreotes, P., and Janetopoulos, C. (2003) Eukaryotic chemotaxis: distinctions between directional sensing and polarization, *J. Biol. Chem. 278*, 20445−8.
24. Rickert, P., Weiner, O. D., Wang, F., Bourne, H. R., and Servant, G. (2000) Leukocytes navigate by compass: roles of PI3Kgamma and its lipid products, *Trends Cell Biol. 10*, 466−73.
25. Gray, A., Olsson, H., Batty, I. H., Priganica, L., and Peter Downes, C. (2003) Nonradioactive methods for the assay of phosphoinositide 3-kinases and phosphoinositide phosphatases and selective detection of signaling lipids in cell and tissue extracts, *Anal. Biochem. 313*, 234−45.
26. Snyder, J. T., Rossman, K. L., Baumeister, M. A., Pruitt, W. M., Siderovski, D. P., Der, C. J., Lemmon, M. A., and Sondek, J. (2001) Quantitative analysis of the effect of phosphoinositide interactions on the function of Dbl family proteins, *J. Biol. Chem. 276*, 45868−75.
27. Klarlund, J. K., Tsiaras, W., Holik, J. J., Chawla, A., and Czech, M. P. (2000) Distinct polyphosphoinositide binding selectivities for pleckstrin homology domains of GRP1-like proteins based on diglycine versus triglycine motifs, *J. Biol. Chem. 275*, 32816−21.
28. Macia, E., Paris, S., and Chabre, M. (2000) Binding of the PH and polybasic C-terminal domains of ARNO to phosphoinositides and to acidic lipids, *Biochemistry 39*, 5893−901.
29. Currie, R. A., Walker, K. S., Gray, A., Deak, M., Casamayor, A., Downes, C. P., Cohen, P., Alessi, D. R., and Lucocq, J. (1999) Role of phosphatidylinositol 3,4,5-trisphosphate in regulating the activity and localization of 3-phosphoinositide-dependent protein kinase-1, *Biochem. J. 337* (Part 3), 575−83.
30. Kavran, J. M., Klein, D. E., Lee, A., Falasca, M., Isakoff, S. J., Skolnik, E. Y., and Lemmon, M. A. (1998) Specificity and promiscuity in phosphoinositide binding by pleckstrin homology domains, *J. Biol. Chem. 273*, 30497−508.
31. Venkateswarlu, K., Gunn-Moore, F., Oatey, P. B., Tavare, J. M., and Cullen, P. J. (1998) Nerve growth factor- and epidermal growth factor-stimulated translocation of the ADP-ribosylation factor-exchange factor GRP1 to the plasma membrane of PC12 cells requires activation of phosphatidylinositol 3-kinase and the GRP1 pleckstrin homology domain, *Biochem. J. 335* (Part 1), 139−46.
32. Frech, M., Andjelkovic, M., Ingley, E., Reddy, K. K., Falck, J. R., and Hemmings, B. A. (1997) High affinity binding of inositol phosphates and phosphoinositides to the pleckstrin homology domain of RAC/protein kinase B and their influence on kinase activity, *J. Biol. Chem. 272*, 8474−81.
33. Klarlund, J. K., Guilherme, A., Holik, J. J., Virbasius, J. V., Chawla, A., and Czech, M. P. (1997) Signaling by phosphoinositide-3,4,5-trisphosphate through proteins containing pleckstrin and Sec7 homology domains, *Science 275*, 1927−30.
34. Takeuchi, H., Kanematsu, T., Misumi, Y., Sakane, F., Konishi, H., Kikkawa, U., Watanabe, Y., Katan, M., and Hirata, M. (1997) Distinct specificity in the binding of inositol phosphates by pleckstrin homology domains of pleckstrin, RAC-protein kinase, diacylglycerol kinase and a new 130 kDa protein, *Biochim. Biophys. Acta 1359*, 275−85.
35. James, S. R., Downes, C. P., Gigg, R., Grove, S. J., Holmes, A. B., and Alessi, D. R. (1996) Specific binding of the Akt-1 protein kinase to phosphatidylinositol 3,4,5-trisphosphate without subsequent activation, *Biochem. J. 315* (Part 3), 709−13.
36. Garcia, P., Gupta, R., Shah, S., Morris, A. J., Rudge, S. A., Scarlata, S., Petrova, V., McLaughlin, S., and Rebecchi, M. J. (1995) The pleckstrin homology domain of phospholipase C-delta 1 binds with high affinity to phosphatidylinositol 4,5-bisphosphate in bilayer membranes, *Biochemistry 34*, 16228−34.
37. Lemmon, M. A., Ferguson, K. M., O'Brien, R., Sigler, P. B., and Schlessinger, J. (1995) Specific and high-affinity binding of inositol phosphates to an isolated pleckstrin homology domain, *Proc. Natl. Acad. Sci. U.S.A. 92*, 10472−6.
38. Rebecchi, M., Peterson, A., and McLaughlin, S. (1992) Phosphoinositide-specific phospholipase C-delta 1 binds with high affinity to phospholipid vesicles containing phosphatidylinositol 4,5-bisphosphate, *Biochemistry 31*, 12742−7.
39. Jackson, T. R., Kearns, B. G., and Theibert, A. B. (2000) Cytohesins and centaurins: mediators of PI 3-kinase-regulated Arf signaling, *Trends Biochem. Sci. 25*, 489−95.
40. Chung, C. Y., Funamoto, S., and Firtel, R. A. (2001) Signaling pathways controlling cell polarity and chemotaxis, *Trends Biochem. Sci. 26*, 557−66.
41. Ridley, A. J., Schwartz, M. A., Burridge, K., Firtel, R. A., Ginsberg, M. H., Borisy, G., Parsons, J. T., and Horwitz, A. R. (2003) Cell migration: integrating signals from front to back, *Science 302*, 1704−9.
42. Laemmli, U. K. (1970) Cleavage of structural proteins during the assembly of the head of bacteriophage T4, *Nature 227*, 680−5.
43. Copeland, R. A. (1994) *Methods for Protein Analysis: A Practical Guide to Laboratory Protocols*, Chapman and Hall, New York.
44. Nalefski, E. A., Slazas, M. M., and Falke, J. J. (1997) Ca2+-signaling cycle of a membrane-docking C2 domain, *Biochemistry 36*, 12011−8.
45. Nalefski, E. A., and Falke, J. J. (2002) Use of fluorescence resonance energy transfer to monitor Ca(2+)-triggered membrane docking of C2 domains, *Methods Mol. Biol. 172*, 295−303.
46. Cozier, G., Sessions, R., Bottomley, J. R., Reynolds, J. S., and Cullen, P. J. (2000) Molecular modelling and site-directed mutagenesis of the inositol 1,3,4,5-tetrakisphosphate-binding pleckstrin homology domain from the Ras GTPase-activating protein GAP1IP4BP, *Biochem. J. 349*, 333−42.
47. Vance, D. E., and Vance, J. E. (2002) *Biochemistry of Lipids, Lipoproteins and Membranes*, 4th ed., Elsevier Science, Boston.
48. Gambhir, A., Hangyas-Mihalyne, G., Zaitseva, I., Cafiso, D. S., Wang, J., Murray, D., Pentyala, S. N., Smith, S. O., and McLaughlin, S. (2004) Electrostatic sequestration of PIP2 on phospholipid membranes by basic/aromatic regions of proteins, *Biophys. J. 86*, 2188−207.

49. Wang, J., Gambhir, A., McLaughlin, S., and Murray, D. (2004) A computational model for the electrostatic sequestration of PI(4,5)P2 by membrane-adsorbed basic peptides, *Biophys. J. 86*, 1969−86.
50. Klarlund, J. K., Rameh, L. E., Cantley, L. C., Buxton, J. M., Holik, J. J., Sakelis, C., Patki, V., Corvera, S., and Czech, M. P. (1998) Regulation of GRP1-catalyzed ADP ribosylation factor guanine nucleotide exchange by phosphatidylinositol 3,4,5-trisphosphate, *J. Biol. Chem. 273*, 1859−62.
51. McLaughlin, S., Wang, J., Gambhir, A., and Murray, D. (2002) PIP(2) and proteins: interactions, organization, and information flow, *Annu. Rev. Biophys. Biomol. Struct. 31*, 151−75.
52. Stephens, L., McGregor, A., and Hawkins, P. (2000) Phosphoinositide 3-kinases: Regulation by cell-surface receptors and function of 3-phosphorylated lipids, in *Biology of Phosphoinositides* (Cockcroft, S., Ed.) pp 32−108, Oxford University Press, Oxford, U.K.
53. Insall, R. H., and Weiner, O. D. (2001) PIP3, PIP2, and cell movement−similar messages, different meanings? *Dev. Cell 1*, 743−7.
54. Hawkins, P. T., Jackson, T. R., and Stephens, L. R. (1992) Platelet-derived growth factor stimulates synthesis of PtdIns(3,4,5)P3 by activating a PtdIns(4,5)P2 3-OH kinase, *Nature 358*, 157−9.
55. Singh, S. M., and Murray, D. (2003) Molecular modeling of the membrane targeting of phospholipase C pleckstrin homology domains, *Protein Sci. 12*, 1934−53.
56. Davis, M. E., Madura, J. D., Sines, J., Luty, B. A., Allison, S. A., and McCammon, J. A. (1991) Diffusion-controlled enzymatic reactions, *Methods Enzymol. 202*, 473−97.
57. Janin, J. (1997) The kinetics of protein−protein recognition, *Proteins 28*, 153−61.
58. White, S. H., and Wimley, W. C. (1998) Hydrophobic interactions of peptides with membrane interfaces, *Biochim. Biophys. Acta 1376*, 339−52.
59. Ladokhin, A. S., and White, S. H. (2001) Protein chemistry at membrane interfaces: nonadditivity of electrostatic and hydrophobic interactions, *J. Mol. Biol. 309*, 543−52.
60. Newton, A. C. (2001) Protein kinase C: structural and spatial regulation by phosphorylation, cofactors, and macromolecular interactions, *Chem. Rev. 101*, 2353−64.
61. Nalefski, E. A., and Newton, A. C. (2001) Membrane binding kinetics of protein kinase C betaII mediated by the C2 domain, *Biochemistry 40*, 13216−29.

BI049017A